Ce_2CuGe_3: A nonmagnetic atom-disorder spin glass

Cheng Tien, Chung Hsing Feng, Ching Shui Wur, and Jenq Jong Lu
Department of Physics, National Cheng Kung University, Tainan, Taiwan, Republic of China
(Received 9 August 1999)

We have studied the magnetic, electric, and thermal properties of Ce_2CuGe_3. The zero-field cooled susceptibility $\chi_{ZFC}(T)$ deviates from the field-cooled susceptibility $\chi_{FC}(T)$ below 3 K, which suggests a spin-glass phase transition at $T_f = 3$ K. The real (χ') and imaginary (χ'') components of the ac susceptibility exhibit pronounced maxima at ~3 K and ~2 K, respectively. At 2 K, the magnetization $M(H)$ clearly exhibits hysteresis. Below 6 K, Ce_2CuGe_3 shows small spontaneous magnetic ordering. The specific heat $C(T)$ of Ce_2CuGe_3 presents a peak ~4 K. Since the magnetic entropy between 2 and 4 K is much smaller than $2R \ln 2$, the 4-K peak of $C(T)$ is unlikely related to a long-range magnetic ordering. This 4-K peak of $C(T)$ might be due to Schottky anomaly with spin-glass contribution. The coefficient of the term linear in temperature in the specific heat γ of Ce_2CuGe_3 is 249.86 mJ mole^{-1} K^{-2}, which is much larger than that of normal metals. A spin-glass magnetism could result in a possible enlargement of the specific heat. At 2 K, the resistance $R(H)$ features hysteresis. This compound might be classified as a nonmagnetic atom-disorder spin glass or a reentrant spin glass.

I. INTRODUCTION

Spin-glass magnetism could be induced to a possible enlargement of specific heat.[1,2] As an example, the γ value of $CePd_3B_{0.3}$ is 0.240 J mole^{-1} K^{-2}, where γ is the coefficient of the term linear in temperature in the specific heat. Gschneidner *et al.*[3] suggested that the enhancement of γ is caused by a spin-glass state that is due to the presence of atomic site disorder. In $CePd_3B_{0.3}$ the B atoms randomly occupy the body-center site of this antiperovskite crystal, which introduces a varying electronic environment around Ce ions and thus causes a variation in the Ruderman-Kittel-Kasuya-Yosida (RKKY) mediated exchange interaction between the Ce ions. The interaction depends upon the boron occupation in the vicinity of Ce ions. It is this random Ce-Ce exchange interaction that gives rise to the spin-glass behavior and this accounts for the large observed γ value. Gschneidner *et al.* called this kind of material a nonmagnetic atom-disorder spin-glass (NMAD spin glass).

The NMAD spin glasses U_2TSi_3 (T = Fe, Co, Ni, Ru, Rh, Pd, Os, Ir, Pt, Au), which crystallize in the hexagonal AlB_2-type structure, were reported by Kaczorowski and Noël.[4] The low-temperature spin-glass behavior in U_2TSi_3 results from the statistical distribution of T and Si atoms at crystallographically equivalent lattice sites, and gives some randomness in U-U exchange interactions.

An NMAD spin glass Ce_2CuSi_3 was reported by Hwang, Lin, and Tien.[5] The specific heat indicates a γ of 152 mJ mole^{-1} K^{-2}. The enhancement of γ may be due to the random-site occupancy of Si and Cu. At a low field (5 Oe), the different temperature dependence of the field-cooled and zero-field-cooled dc susceptibilities suggests a spin-glass state in Ce_2CuSi_3 below 9 K.

Replacing Si by Ge in Ce_2CuSi_3 is similar to applying a negative ''chemical pressure.'' The negative pressure will increase the site disorder. Therefore, the spin-glass behavior might be more explicit in Ce_2CuGe_3 than those in Ce_2CuSi_3. In this paper we report on the magnetic, electric, and thermal properties of Ce_2CuGe_3. The spin-glass-like behavior of Ce_2CuGe_3 is compared to the properties of canonical spin glasses and other NMAD spin glasses.

II. EXPERIMENTAL RESULTS

Polycrystalline samples of Ce_2CuGe_3 and La_2CuGe_3 were prepared by the arc melting of the pure elements in their stoichiometric ratio in an atmosphere of purified argon gas. The button was flipped over the remelted a number of times to achieve good homogeneity. The overall weight loss during the melting was less than 1%. X-ray measurements of the sample were carried out at room temperature and showed only a single phase. Figure 1 shows the x-ray diffraction patterns of Ce_2CuGe_3 and La_2CuGe_3. The crystal structure of Ce_2CuGe_3 and La_2CuGe_3 can be described in an orthorhombic cell with $(b, c \cong a/\sqrt{3})$. Where $a = 7.262$ Å, $b = 4.591$ Å, and $c = 4.231$ Å for Ce_2CuGe_3; $a = 7.260$ Å, $b = 4.608$ Å, and $c = 4.465$ Å for La_2CuGe_3.

The dc magnetic properties were measured by a quantum design SQUID (superconducting quantum-interference device) magnetometer. Figure 2 is the zero-field-cooled molar susceptibility (χ_{ZFC}) and field-cooled molar susceptibility (χ_{FC}) of Ce_2CuGe_3 between 2 and 30 K at 10 Oe. For ZFC we cooled the sample from 300 to 2 K in the zero field and applied the field at 2 K. (By the low-field profiling option of quantum design, we can measure the remnant field at the sample position. Without the applied field, the magnetic field at the sample position is ~0.4 Oe.) Then we heated the sample while measuring the χ in the constant field. For FC, the sample was cooled in a magnetic field from 300 to 2 K and then it was heated up while measuring the χ. The inset of Fig. 2 is the temperature dependence of the inverse of susceptibility, $1/\chi_{ZFC}$ between 2 and 300 K at 10 Oe. As shown in the inset of Fig. 2, the susceptibility of Ce_2CuGe_3 follows Curie-Weiss law above 30 K. Below this temperature, a negative deviation appears with a negative Curie-Weiss tem-

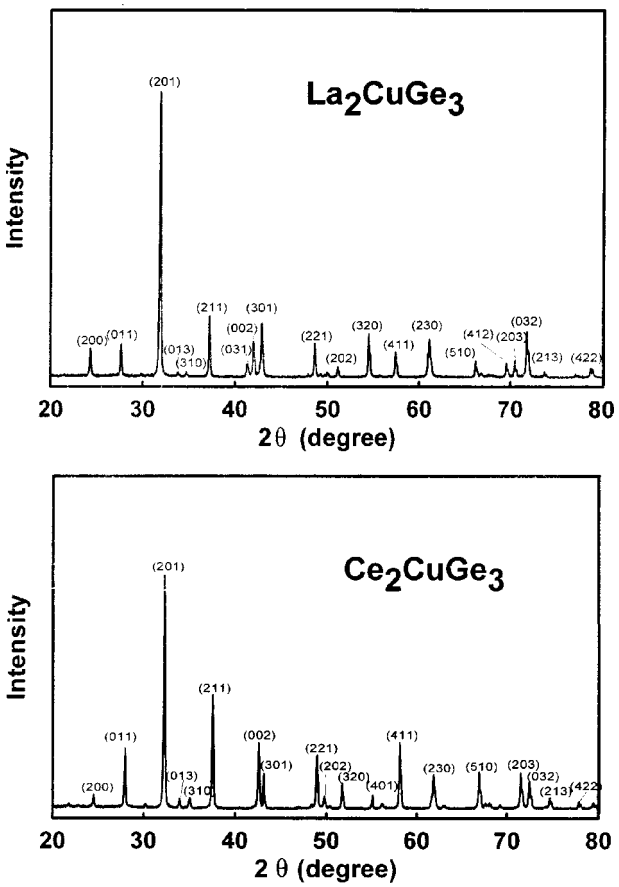

FIG. 1. The x-ray diffraction patterns of Ce_2CuGe_3 and La_2CuGe_3. The program we used to index x-ray diffraction data of Ce_2CuGe_3 and La_2CuGe_3 is XARYSCAN (Ref. 6).

perature $\theta = -10.4$ K. The effective moment deduced from the paramagnetic region is $2.38\mu_B$ which is in agreement with the theoretical value of Ce^{3+} free atom at $^2F_{5/2}$ state ($2.54\mu_B$). As shown in Fig. 2, below 3 K, the temperature dependence of χ_{ZFC} and χ_{FC} is different. There is a peak at 2.2 K in $\chi_{ZFC}(T)$. Figures 3 and 4 are the temperature de-

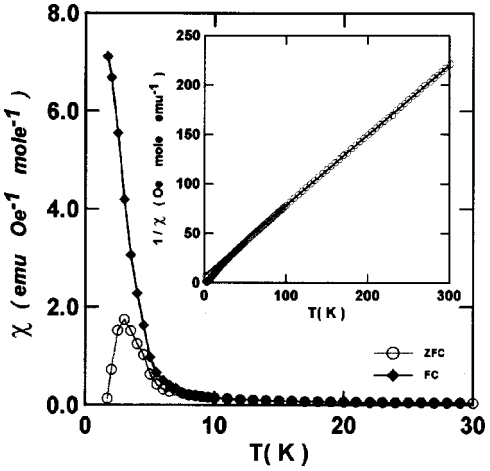

FIG. 2. The temperature dependence of zero-field-cooled susceptibility $\chi_{ZFC}(\bigcirc)$ and field-cooled susceptibility $\chi_{FC}(\blacklozenge)$ of Ce_2CuGe_3 between 2 and 30 K at 10 Oe. The inset is $1/\chi_{ZFC}(T)$ between 2 and 300 K.

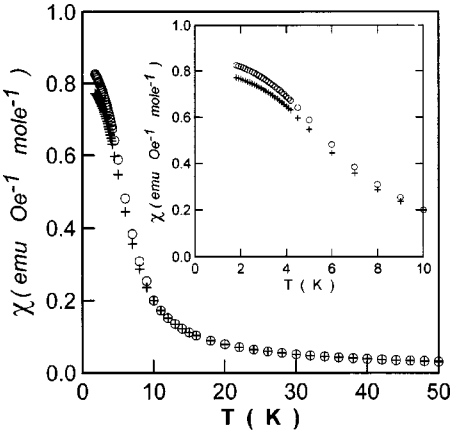

FIG. 3. The temperature dependence of zero-field-cooled susceptibility $\chi_{ZFC}(+)$ and field-cooled susceptibility $\chi_{FC}(\bigcirc)$ of Ce_2CuGe_3 between 2 and 50 K at 1 T. The inset is χ_{ZFC} and χ_{FC} between 2 and 10 K.

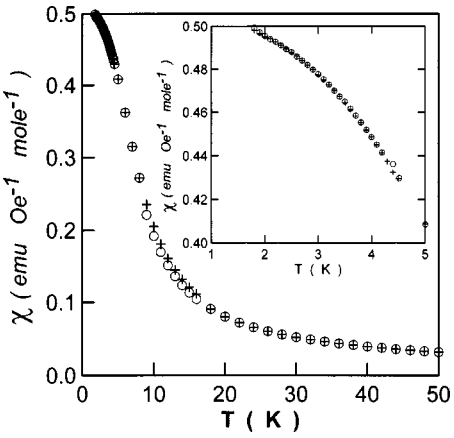

FIG. 4. The temperature dependence of zero-field-cooled susceptibility $\chi_{ZFC}(+)$ and field-cooled susceptibility $\chi_{FC}(\bigcirc)$ of Ce_2CuGe_3 between 2 and 50 K at 2 T. The inset is χ_{ZFC} and χ_{FC} between 2 and 5 K.

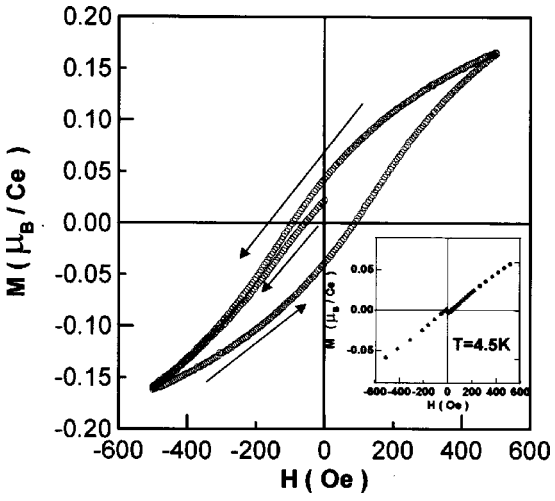

FIG. 5. The field dependence of magnetization $M_{ZFC}(H)$ for Ce_2CuGe_3 at 2 K. The inset is $M_{ZFC}(H)$ at 4.5 K.

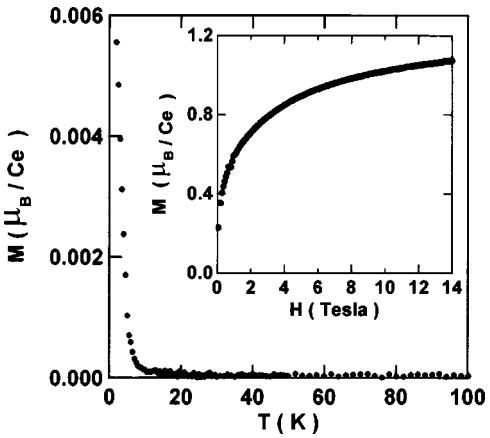

FIG. 6. The spontaneous magnetic ordering of Ce_2CuGe_3 at 2 K. The inset is the field dependence of magnetization $M(H)$ between 0 and 14 T.

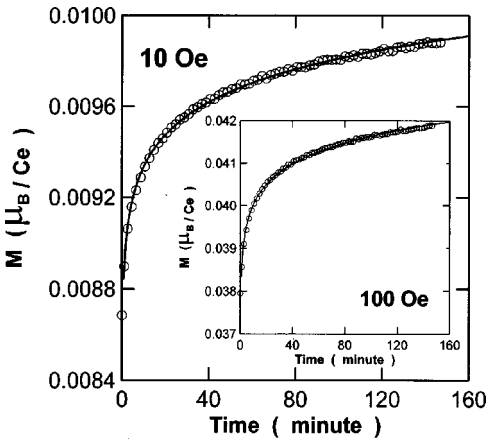

FIG. 7. The time dependence of magnetization $M_{ZFC}(t)$ for Ce_2CuGe_3 at 2 K in 10 Oe. The solid curve is the fitting curve of $M_{ZFC}(t)=M_0-M'\exp[(-t/\tau)^{1-n}]$. The fitting values are indicated in Table I. The inset is the $M_{ZFC}(t)$ in 100 Oe.

pendence of of χ_{ZFG} and χ_{FC} at high magnetic fields. As shown in Fig. 3, at 1 T, the peak of χ_{ZFC} vanishs and the χ_{FC} slightly deviates from χ_{ZFC} below 6 K. When the field is higher than 2 T, there is no difference between χ_{ZFC} and χ_{FC} (Fig. 4).

Figure 5 is the magnetization vs the magnetic field $M(H)$ at 2 and 4.5 K. At 2 K, $M(H)$ clearly exhibits hysteresis. Although the magnetic curves clearly deviate from a linear relationship between M and H, there is no hysteresis and remnant magnetization at 4.5 K.

To confirm further the magnetization hysteresis in Ce_2CuGe_3, we measured the magnetization $M(T)$ without any applied field. As shown in Fig. 6, at zero applied field, $M(T)$ indicates a very small spontaneous magnetic ordering below 6 K. The inset of Fig. 6 is the field dependence of magnetization $M(H)$ at 2 K, even at 14 T $M(H)$ is still not saturated. Therefore, it is unlikely that the small spontaneous magnetic ordering in Ce_2CuGe_3 below 6 K is due to ferromagnetic impurity or second-phase contamination.

In a spin-glass state, it takes several decades to turn the magnetic moments toward the field direction. Figure 7 shows the time dependence of zero-field-cooled magnetization $M_{ZFC}(t)$ at 2 K in a 10 Oe field. Even progressing for 2 h, $M_{ZFC}(t)$ remains unsaturated. The solid line in Fig. 7 is the fitting curve of the stretched exponential function:

$$M_{ZFC}(t)=M_0-M'\exp\left[\left(\frac{t}{\tau}\right)^{1-n}\right]$$

with $\tau=1800$ sec. As shown in the inset of Fig. 7, the magnetic field will significantly reduce the τ value; in a 100 Oe field τ is 1030 sec. The fitting values of the stretched exponential function in 10 and 100 Oe field are indicated in Table I.

The ac magnetic properties were measured by a quantum design PPMS (physical property measurement system). The ac susceptibilities of Ce_2CuGe_3 are studied in ac fields 1 Oe at 100 Hz, 1000 Hz, and 10 000 Hz. As shown in Fig. 8, both the real (χ') and imaginary (χ'') components of the susceptibility exhibit pronounced maxima.

The specific-heat measurements were performed in a quantum design PPMS by a modified heat-pulse method.[7] Figure 9 shows the specific heat vs temperature $C(T)$ of Ce_2CuGe_3. There is a peak in $C(T)$ at 4 K. By susceptibility measurements, there is no magnetic transition at 4 K. The 4-K peak might be caused by crystal-field splitting. Between 35 and 25 K, the $C(T)$ of Ce_2CuGe_3 can be described by $C(T)=\gamma_1 T+\beta_1 T^3$ with $\gamma_1=200.58$ mJ/mol K^2 and $\beta_1=0.748$ mJ/mol K^4. Below 35 K the $C(T)$ of La_2CuGe_3 can be described by $C(T)=\gamma_2 T+\beta_2 T^3$ with $\gamma_2=4.87$ mJ/mol K^2 and $\beta_2=0.737$ mJ/mol K^4. The magnetic specific heat is defined here as $C_m(T)=C(Ce_2CuGe_3)-C(La_2CuGe_3)$. Between 20 and 35 K, $C_m(T)/T$ can be fitted by $\gamma_m+\beta_m T^2$ with $\gamma_m=116$ mJ/mol K^2 and $\beta_m=0.011$ mJ/mol K^4.

Electrical resistivity is measured by a four-probe method. The electrical resistivities of $\rho(T)$ of Ce_2CuGe_3 and La_2CuGe_3 between 4.2 and 300 K are shown in Fig. 10. The $\rho(T)$ of Ce_2CuGe_3 and La_2CuGe_3 exhibits a linear dependence of temperature over a broad temperature range. The resistivity of Ce_2CuGe_3 moderately deviates from linearity around 100 K with a peak at 7.3 K.

III. DISCUSSION

The deviation of $\chi_{FC}(T)$ from $\chi_{ZFC}(T)$ suggests that below 3 K, there is a spin-glass state in Ce_2CuGe_3. The x-ray

TABLE I. The fitting values of $M_{ZFC}(t)=M_0-M'\exp[(-t/\tau)^{1-n}]$.

Field (Oe)	10	100
M_0 (μ_B/Ce)	$1.017\times10^{-2}\pm2.0\times10^{-5}$	$4.237\times10^{-2}\pm4.2\times10^{-5}$
M' (μ_B/Ce)	$1.567\times10^{-3}\pm2.8\times10^{-5}$	$5.311\times10^{-3}\pm8.5\times10^{-5}$
τ (sec)	$1.800\times10^{3}\pm97.79$	$1.030\times10^{3}\pm37.75$
n	$0.647\,6\pm0.007\,086$	$0.606\,6\pm0.008\,448$

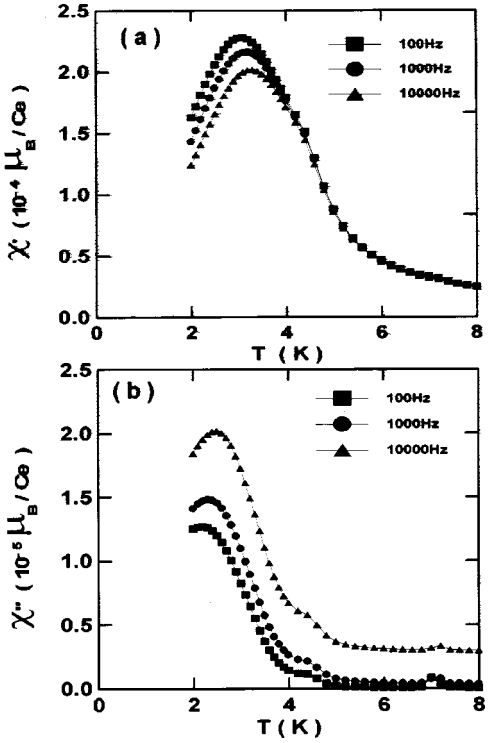

FIG. 8. (a) The temperature dependence of real component of the ac susceptibility (χ') for Ce_2CuGe_3 in an ac field 1 Oe at 100, 1000, 10 000 Hz, (b) imaginary component of the ac susceptibility (χ'').

diffraction lines of Ce_2CuGe_3 cannot be indexed by a hexagonal structure. Although when T = Fe, Co, Ni, Ru, Rh, Pd, Os, Ir, Pt, U_2TSi_3 crystallizes in the hexagonal AlB_2-type structure, an orthorhombic cell is observed for U_2RhSi_3 by Chevalier *et al.*[8] If Ce_2CuGe_3 has the same crystal structure as U_2RhSi_3, Ce^{3+} ions are located on layers separated by sheets of Ge and Cu atoms. The possible mechanism of the spin glass in Ce_2CuGe_3 is that the magnetic moments of Ce^{3+} ions on the same layer form a ferromagnetic order, but different Ce^{3+} layers correlate antiferromagnetically. Therefore, the combination of the site randomness of Cu and Ge ions with competing ferromagnetic and antiferromagnetic interactions between Ce ions cause the spin-glass phase in Ce_2CuGe_3. Suppose Ce_2CuGe_3 has the same crystal structure as U_2RhSi_3, the calculated line intensities are given in Table II. As shown in Table II, there is a reasonable agreement between observed I_{obs} and calculated line intensities I_{calc}. Since the x-ray diffraction lines of powdered samples are not suitable for intensity analysis, I_{obs} somewhat deviates from I_{calc}. However, the deviation of I_{obs} from I_{calc} might be also due to the random distribution of Cu and Ge atoms at crystallographically equivalent lattice site. However, the x-ray diffraction spectrum of a single-crystal Ce_2CuGe_3 is needed to clarify the crystal structure of Ce_2CuGe_3.

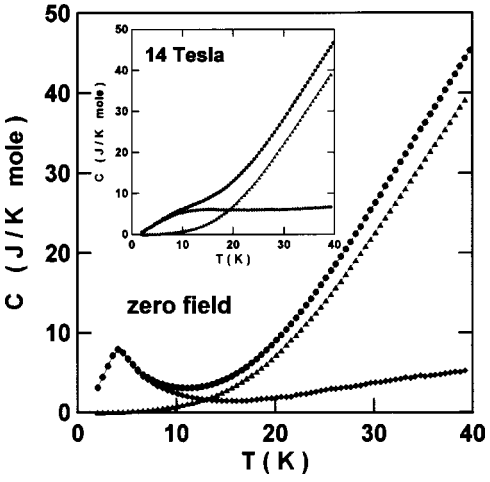

FIG. 9. The temperature dependence of specific heat $C(T)$ of Ce_2CuGe_3 (●) and La_2CuGe_3 (▲). The magnetic specific heat $C_m(T)$ (♦) is defined as $C_m(T)=C(Ce_2CuGe_3)-C(La_2CuGe_3)$. The inset is $C(T)$ and $C_m(T)$ in 14 T.

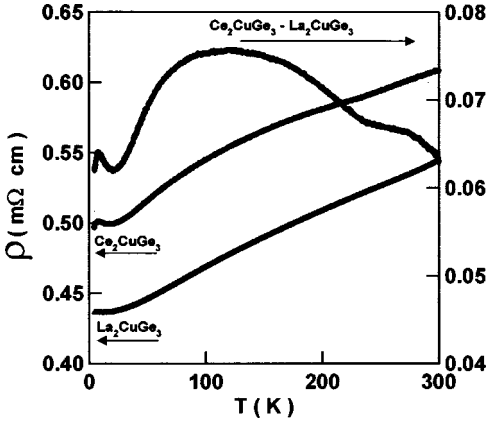

FIG. 10. The electrical resistivity of Ce_2CuGe_3 and La_2CuGe_3. The $\rho_m(T)$ is $\rho(Ce_2CuGe_3)-\rho(La_2CuGe_3)$.

In a spin glass, the spin freezing temperature T_f can be identified as a temperature where the field-cooled and zero-field-cooled dc susceptibilities meet. Therefore, the T_f of

TABLE II. Comparison of the calculated and observed line intensity for Ce_2CuGe_3.

$h\,k\,l$	I_{calc}	I_{obs}
200	9	5
011	13	25
201	100	100
013	1	4
310	2	4
211	27	50
002	16	26
301	5	13
221	21	22
202	6	5
320	8	12
401	5	7
411	10	28
230	8	13
510	9	15
203	5	13
032	6	8
213	<1	3
422	2	1

Ce_2CuGe_3 is ~3 K. For a canonical spin glass, for example, CuMn (containing 1 or 2% Mn), below T_f, $\chi_{FC}(T)$ becomes constant of temperature and independent of time to a great extent.[9] However, for Ce_2CuGe_3, below T_f, when the temperature decreases, $\chi_{FC}(T)$ increases rapidly. Therefore, it might have a magnetic-field-induced ferromagnetic phase transition below 2 K.

Since $T_f = 3$ K, the thermal disorder energy $k_B T_f$ of a Ce^{3+} ion in the spin-glass phase is 4.14×10^{-23} J. If the magnetic energy $\mu_{\text{eff}} H$ of a Ce^{3+} ion in an external field H is larger than the thermal disorder energy, the spin-glass phase will disappear. The effective magnetic moment of a Ce^{3+} ion in Ce_2CuGe_3 is $\mu_{\text{eff}} = 2.38\mu_B$. Therefore, if H is larger than a critical field $H_c = 1.876$ T, $\chi_{ZFC}(T) = \chi_{FC}(T)$. As shown in Figs. 3 and 4, $\chi_{ZFC}(T)$ deviates from $\chi_{FC}(T)$ in 1 T but there is no difference between $\chi_{ZFC}(T)$ and $\chi_{FC}(T)$ in 2 T. It is suggested that $1 < H_c < 2$ T, which agrees with the above argument.

However, the deviation of $\chi_{FC}(T)$ from $\chi_{ZFC}(T)$ alone cannot conclude a spin-glass state at low temperature. For example, although in U_2RhSi_3, $\chi_{FC}(T)$ deviates from $\chi_{ZFC}(T)$ below 10.4 K, a spin-glass-type transition is not observed in an ac susceptibility measurement.[8] Chevalier *et al.*[8] claimed that the difference of $\chi_{FC}(T)$ from $\chi_{ZFC}(T)$ in U_2RhSi_3 is a result of ferromagnet displaying noticeable domain-wall pinning effect instead of a spin-glass phase.

As it is well known in the case of alloys that undergo a paramagnetic to a spin-glass transition as a function of decreasing temperature, the real (in phase) component of magnetic ac susceptibility χ' exhibits a cusp at the spin freezing temperature T_f. For example, for measured frequency 234 Hz and applied oscillating field$\leqslant$1 Oe, the real part of the ac susceptibility of a canonical spin glass AuMn, χ', exhibits a sharp maximum at $T_f \sim 10.2$ K.[10] Although no peak is observed in χ'', a pronounced anomaly in χ'' is observable around 10.2 K. Furthermore, the maximum in $|d\chi''(T)/dT|$ nicely coincides with the maximum of χ'. A similar behavior of χ'' was also observed in CuMn.[11]

The ac susceptibility of a spin-glass compound U_2CoSi_3 was reported by Kaczorowski and Noël.[4] Both the real and imaginary components of the susceptibility show pronounced maxima. The susceptibility maxima of χ' and χ'' for U_2CoSi_3 are not cusped but rather rounded. Besides, the maxima of χ' and χ'' occur at slightly different temperature. Kaczorowski and Noël claimed that U_2CoSi_3 is not a simple spin glass but a re-entrant spin glass, exhibiting first ferromagnetic transition at 10 K and then showing spin-glass properties below about 8 K.

As shown in Fig. 8, the real (χ') and imaginary (χ'') components of the ac susceptibility exhibit pronounced maxima at ~3 K and ~2 K, respectively. The effective moment of each Ce^{3+} ion is $\mu_{\text{eff}} = 2.4\mu_B$. The peak of χ' for Ce_2CuGe_3 is too broad and the peak value $\sim 2.3 \times 10^{-4} \mu_B$/Ce is too small for a conventional ferromagnetic ordering. If the spin freezing temperature T_f is defined as maximum in the χ', the frequency dependence is extremely small for Ce_2CuGe_3 ($\Delta T_f = 0.2$ K for $\Delta \nu = 10^4$ Hz); therefore the relative shift in freezing temperature per decade of frequency

$$\frac{\Delta T_f}{T_f(\Delta \log_{10} \nu)} = 0.016.$$

Although the frequency shift of T_f for Ce_2CuGe_3 is larger than that (0.005) for a canonical spin glass CuMn (Ref. 12), it is still much smaller than that for a superparamagnet.[13]

In Ce_2CuGe_3, the imaginary (χ'') component of the susceptibility is one order of magnitude smaller than the real (χ') component. Since peaks of χ' and χ'' occur at slightly different temperatures, the peak of χ'' at ~2 K might correspond to a magnetic transition. As shown in Fig. 2, χ_{ZFC} deviates from χ_{FC} below 3 K and has a peak at 2.2 K, which further supports a spin-glass transition at ~3 K and then a magnetic transition at ~2 K. A further experiment, for example, neutron scattering, is needed to clarify these unusual properties of Ce_2CuGe_3.

As shown in Fig. 5, the $M(H)$ of Ce_2CuGe_3 exhibits magnetization hysteresis at 2 K. The magnetization hysteresis could result from the motion of ferromagnetic domain walls or the time dependence of $M(H)$ in a spin-glass state. As shown in Fig. 8(b), the peak of χ'' shows clear frequency dependence. The frequency shift of χ'' means relaxation processes are affecting the measurement and by decoupling the spins from the lattice they cause the absorption.[13] Usually the frequency dependence of Néel temperature for a long-range ferromagneticism can be observed only if the frequency is higher than 10^6 Hz. The low-frequency dependence of χ'' suggests that the hysteresis of Ce_2CuGe_3 at low temperature should be due to a spin-glass phase instead of a long-range ferromagnetic order.

In Ce_2CuGe_3, Ce ions are located on layers separated by sheets of transition metal and Ge atoms. The magnetic moments of Ce ions on the same layer form a ferromagnetic order, but different Ce layers correlate antiferromagnetically. If there is a small amount of random mixed crystallographic site between Cu and Ge in Ce_2CuGe_3, the electronic environment around the Ce ion will be varied, which will cause a variation in the RKKY mediated exchange interaction between the Ce ions. The competition of randomly distributed ferromagnetic and antiferromagnetic interactions might develop ferromagnetic clusters—the building blocks out of which the spin-glass state is established.[13] These clusters may be coupled resulting a spin frozen state.

In a spin-glass state or a spin frozen state, it takes several decades to turn the magnetic moments toward the field direction. The time constant of $M_{ZFC}(t)$ at 2 K in 10 Oe is 1800 sec, which is long enough to suggest a spin frozen state in Ce_2CuGe_3 below 2 K.

As shown in the inset of Fig. 5, the nonlinear relationship between magnetization and magnetic field $M(H)$ appears at 4.5 K, which is above $T_f = 3$ K. This behavior can also be explained by the spin-glass phase in Ce_2CuGe_3. The competition of ferromagnetic and antiferromagnetic interactions will create ferromagnetic clusters in Ce_2CuGe_3. The cooperation between ferromagnetic clusters starts at T_f, but the ferromagnetic clusters might occur above T_f. It is the ferromagnetic clusters which cause the nonlinear behavior of $M(H)$ above $T_f = 3$ K.

The γ of Ce_2CuGe_3 is much larger than those of normal metals. A spin-glass magnetism could result in a possible enlargement of the specific heat.[14,15] The possible mecha-

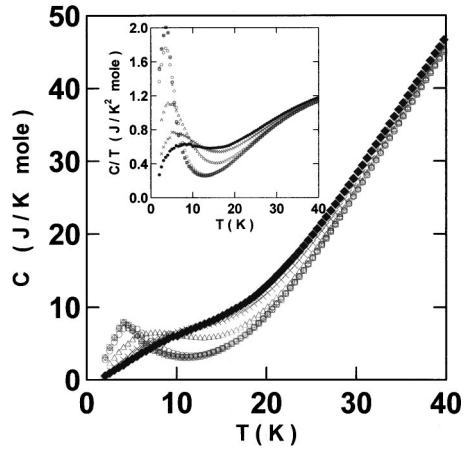

FIG. 11. The specific heat vs temperature $C(T)$ of Ce_2CuGe_3 between 2.5 and 40 K in 0, 0.01, 0.1, 1, 5, 10, and 14 T. The inset is $C(T)/T$ in 0, 0.01, 0.1, 1, 5, 10, and 14 T.

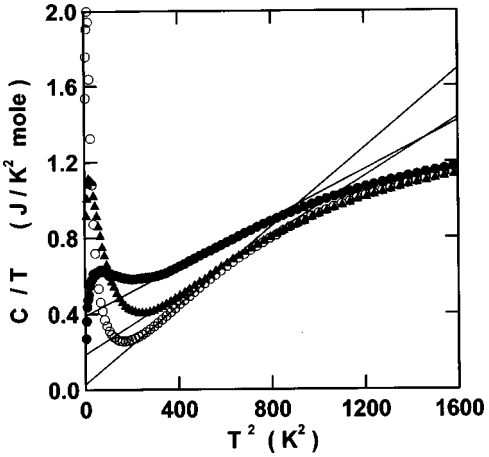

FIG. 12. The $C(T)/T$ vs T^2 of Ce_2CuGe_3 in 0 (○), 5 (▲), and 14 (●) T.

nisms that will enhance the γ value are (1) low lying crystal levels, (2) a spin-glass phase, and (3) magnetic ordering at low temperature.

By susceptibility measurements, there is no magnetic transition at 4 K. The simplest interpretation of these 4-K peaks of $C(T)$ for Ce_2CuGe_3 (Fig. 9) is due to low lying crystal levels, since the $J=\frac{5}{2}$ multiplet of Ce^{3+} in lattice symmetry lower than cubic splits into three doublets. If the splitting Δ between the ground state and the first excited crystal-field (CF) doublet is much smaller than those of higher excited states, the molar specific heat due to Schottky contribution is[16]

$$C(T)=nR\frac{(\Delta/T)^2e^{\Delta/T}}{(1+e^{\Delta/T})^2},$$

where R is the gas constant and $n=2$ for Ce_2CuGe_3. Therefore, $C(T)$ has a maximum equal to $0.86R$ at $T_{\max}=0.416\Delta$. If $T_{\max}$ is ~4 K, Δ is ~10 K. At 4 K, the magnetic specific heat $C_m(T)$ of Ce_2CuGe_3 is ~8 J/mole K that equals $0.97R$, which is slightly larger than $0.86R$. Therefore, the Schottky contribution alone is somewhat small to explain the enhancement of $C(T)$ at 4 K.

For a canonical spin glass 2790 ppm CuMn, $C(T)$ exhibits a peak at $T_{\max}\sim 5$ K. The spin freezing temperature of CuMn is $T_f\sim 3$ K, such that $T_{\max}\sim 1.4T_f$.[17] When an external magnetic field H is applied, the maximum of $C(T)$ becomes less pronounced and disappears as $H>7.5$ T.

The inset of Fig. 9 shows the specific heat vs temperature $C(T)$ of Ce_2CuGe_3 in 14 T. The magnetic specific heat is $C_m(T,H=14\,\mathrm{T})=C(Ce_2CuGe_3,H=14\,\mathrm{T})-C(La_2CuGe_3,H=14\,\mathrm{T})$. In a 14-T field, the 4-K peak of $C(T)$ is entirely depressed. Figure 11 shows the specific heat vs temperature $C(T)$ of Ce_2CuGe_3 between 2.5 and 40 K at 0, 0.01, 0.1, 1, 5, 10, and 14 T. Below 1 T, the specific heat of Ce_2CuGe_3 is independent of magnetic field. At 5 T, the maximum of $C(T)$ becomes significantly less pronounced and disappears as $H>10$ T. There is still a lack of persuasive theory to calculate the specific heat due to spin-glass order in a NMAD spin glass. Although, the field dependence of the specific heat seems to support the existence of a spin-glass phase, we still cannot rule out the possible contribution of a CF in Ce_2CuGe_3.

The C/T vs T^2 of Ce_2CuGe_3 at 0, 5, and 14 T are shown in Fig. 12. Between 16 and 30 K, the $C(T)$ of Ce_2CuGe_3 can be described by $C(T)=\gamma T+\beta T^3$. The fitting values γ and β in various fields are indicated in Table III. In a 14-T field, the γ value is 437 mJ/mol K^2, which is much larger than those of ordinary metals. In a canonical spin glass, although magnetic clusters correlate as temperature below T_f, they might appear far above the T_f. It is the order of the magnetic clusters that enhances the γ value with increasing of magnetic field. The C/T vs T of Ce_2CuGe_3 in various magnetic fields is

TABLE III. The fitting values of specific-heat coefficients γ and β at 0, 0.01, 0.1, 1, 5, 10, and 14 T. $T_{\max}$ is the temperature, at which C/T shows a peak. S_1 is the magnetic entropy between 2.5 K and $T_{\max}$. S_2 is the magnetic entropy between $T_{\max}$ and 40 K.

Field (T)	γ (mJ/mole K^2)	β (mJ/mole K^4)	S_1 (J K^{-1} mole^{-1})	S_2 (J K^{-1} mole^{-1})	S_1+S_2 (J K^{-1} mole^{-1})	$T_{\max}$
0	200.40	0.748	1.932	9.105	11.037	3.56
0.01	209.08	0.729	1.927	9.086	11.013	3.56
0.1	198.28	0.745	1.927	9.097	11.024	3.56
1	206.20	0.730	1.713	9.432	11.145	3.56
5	260.59	0.684	1.564	10.561	12.125	4.07
10	361.35	0.608	1.605	10.744	12.349	5.05
14	436.97	0.562	1.737	10.653	12.390	6.06

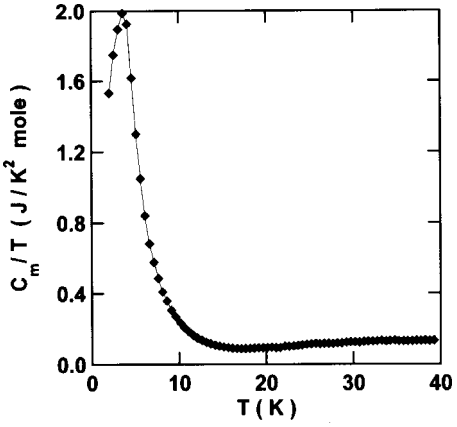

FIG. 13. The $C_m(T)/T$ vs T of Ce_2CuGe_3.

exhibited in the inset of Fig. 11. The C/T shows a peak at T_{max} and a minimum at T_{min}. Above a character temperature $T' \sim 40$ K, C/T is magnetic-field independent. The T_{max} for various fields are indicated in Table III. As shown in the inset of Fig. 11, when $H \geqslant 5$ T, the peak of $C(T)/T$ is significantly depressed by the magnetic field, which suggests a antiferromagnetic-type order below T_{max}. However, as shown in Table III, T_{max} slightly increases as the magnetic field increases, which suggests a ferromagnetic-type order below T_{max}. Therefore the peak of $C(T)/T$ of Ce_2CuGe_3 might be related to a short-range spin-glass order instead of a long-range magnetic order.

For a short-range spin-glass order, T_{max} of C/T might related to the cooperation among magnetic clusters. T' and T_{min} of C/T might relate to the appearance of magnetic clusters in Ce_2CuGe_3. The minimum temperatures T_{min} much higher than T_f further support magnetic clusters that appear far above the T_f. Further experiments, for example, neutron scattering, are needed to clarify these unusual properties of Ce_2CuGe_3.

For a canonical spin glass at low temperature it is shown that entropy is shifted from the low-temperature to the high-temperature portion because a great deal of the magnetic entropy is lost or frozen out far above T_f. For further confirming the spin-glass order in Ce_2CuGe_3, we measure the magnetic entropy of Ce_2CuGe_3.

Figure 13 shows the C_m/T vs T of Ce_2CuGe_3 without magnetic field. The temperatures of our specific-heat measurements are not low enough to determine the entropy accurately. A rough estimate of the magnetic entropy is 11.04 $J\,K^{-1}\,mole^{-1}$, which is close to $2R\ln 2 = 11.53$ $J\,K^{-1}\,mole^{-1}$. If T_{max} is defined as the temperature at which C_m/T has the maximum value and S_1 and S_2 are defined as

$$S_1 = \int_{2.5\,K}^{T_{max}} \frac{C_m}{T} dT \quad \text{and} \quad S_2 = \int_{T_{max}}^{40\,K} \frac{C_m}{T} dT.$$

Then for Ce_2CuGe_3 without magnetic field, $S_1 = 1.93$ $J\,K^{-1}\,mole^{-1}$ and $S_2 = 9.11$ $J\,K^{-1}\,mole^{-1}$. The S_1 and S_2 for various fields are indicated in Table III. As shown in Table III, $S_1 + S_2 \sim 2R\ln 2$ $J\,K^{-1}\,mole^{-1}$, and S_1 is slightly reduced and S_2 is slightly increased by the magnetic field. Therefore, we did not observe a significant shift of the magnetic entropy from the low-temperature to the high-temperature portion by the applied field. Without the applied field, S_1 is 1.932 $J\,K^{-1}\,mole^{-1}$ such that the peak of $C(T)/T$ is unlikely due to second-phase contamination. $S_1 \ll 2R\ln 2$ $J\,K^{-1}\,mole^{-1}$ further supports that the transition at T_{max} (~ 4 K) should not correlate to a long-range-type magnetic order. The small magnetic entropy S_1 between 2.5 and T_{max} ($S_1 = 1.932$ $J\,K^{-1}\,mole^{-1} \ll 2R\ln 2$) is consistent with a spin-glass phase at low temperature.

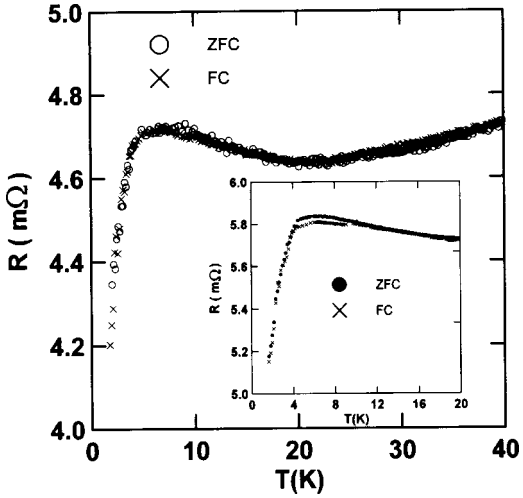

FIG. 14. The zero-field-cooled resistance $R_{ZFC}(T)$ and field-cooled resistance $R_{FC}(T)$ in 1.5 T between 2 and 40 K. The inset is $R_{ZFC}(T)$ and $R_{FC}(T)$ in 200 Oe.

The resistivity may be regarded as the consequence from the following contribution:

$$\rho(T) = \rho_{ph}(T) + \rho_m(T),$$

where $\rho_{ph}(T)$ is the contribution due to the electron-phonon interaction, and the other scattering mechanisms are contained in $\rho_m(T)$. Since in the specific heats the lattice contributions of Ce_2CuGe_3 and La_2CuGe_3 are roughly identical, $\rho_{ph}(T)$ of both compounds might be also the same. Therefore, the magnetic resistivity of Ce_2CuGe_3

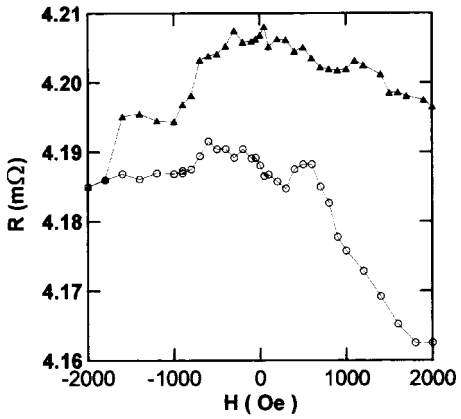

FIG. 15. The field dependence of $R(H)$ at 2 K. The sample was cooled from 300 to 2 K in zero field and applied 2000-Oe field at 2 K. The $R(H)$ was measured from 2000 Oe to -2000 Oe (▲) and than back to 2000 Oe (○).

$$\rho_m(T) \simeq \rho(Ce_2CuGe_3) - \rho(La_2CuGe_3).$$

As shown in Fig. 10, $\rho_m(T)$ rises with decreasing temperature, which might be due to the Kondo effect, and a sharp drop results from the formation of coherent Kondo state at around 7.34 K. A similar behavior was observed in Ce_2CuSi_3 by Hwang *et al.*[5]

In Ce_2CuGe_3, the Ce atoms form a fully periodic lattice, but Cu and Ge exhibit disorder in the arrangement in a unit cell. It is this varying electronic environment around the Ce atoms that introduces the Kondo-like behavior in $\rho_m(T)$. The varying electronic environment around the Ce atoms will produce ferromagnetic clusters at low temperature. If the ferromagnetic cluster is frozen in a spin-glass system, it takes a long time to turn the magnetic moments toward the field direction. However, the ordering of ferromagnetic clusters might reduce the resistance. If the argument is correct, the zero-field-cooled resistance $R_{ZFC}(T)$ is different from the field-cooled resistance $R_{FC}(T)$ when the ferromagnetic clusters are formed. Figure 14 is the zero-field-cooled resistance $R_{ZFC}(T)$ and field-cooled resistance $R_{FC}(T)$ in 1.5 T between 2 and 40 K. The inset of Fig. 14 is $R_{ZFC}(T)$ and $R_{FC}(T)$ in 200 Oe. The current for measuring the resistance is parallel to the direction of the magnetic field. In 200 Oe, $R_{ZFC}(T)$ deviates from $R_{FC}(T)$ at $\sim$12 K, which is higher than $T_f = 4$ K. The deviation of $R_{ZFC}(T)$ from $R_{FC}(T)$ in 200 Oe might be due to the ferromagnetic clusters in a spin glass. As shown in Table I, the magnetic field will significantly reduce the τ value. In a 1.5-T field, τ is too small to indicate the difference between $R_{ZFC}(T)$ and $R_{FC}(T)$. Figure 15 is the field dependence of $R(H)$ at 2 K. We cooled the sample from 300 to 2 K in zero field and applied a 2000-Oe field at 2 K. Then we swept the field from 2000 Oe to -2000 Oe and then back to 2000 Oe. The resistance was measured in the magnetic field. The hysteresis of $R(H)$ further confirms a spin-glass phase in Ce_2CuGe_3.

IV. SUMMARY

In Ce_2CuGe_3, (1) $\chi_{FC}(T)$ deviates from $\chi_{ZFC}(T)$ below 3 K, (2) the real component (χ') of the ac susceptibility exhibits a frequency-dependent maximum at $\sim$3 K, (3) the zero-field-cooled magnetization $M_{ZFC}(t)$ is frozen at 2 K in a 100-Oe field with a time constant 1030 sec, and (4) the magnetic entropy below 4 K is much less than $2R \ln 2$, which suggests a spin-glass phase below 3 K.

Furthermore, (1) at 2 K, the magnetization $M(H)$ clearly exhibits hysteresis; (2) below 6 K, Ce_2CuGe_3 shows small spontaneous magnetic ordering; and (3) below 3 K, $\chi_{FC}(T)$ increases rapidly with decreasing temperature, which suggests a ferromagnetic-type order below 2 K.

Therefore, in Ce_2CuGe_3 spin-glass phase not only stops but persists in a ''ferromagnetic-type phase.'' This seems to suggest that Ce_2CuGe_3 might not be a simple spin glass but a re-entrant spin glass. The temperature at the maximum of $\chi''(T)$ is lower than that at the maximum of $\chi(T)$, which further supports that Ce_2CuGe_3 is a re-entrant spin glass.

The magnetic specific heat $C_m(T)$ of Ce_2CuGe_3 has a maximum $\sim 0.97R$ at $T_{max} = 0.416\Delta$, which is slightly larger than $0.86R$. Therefore, this 4-K peak of $C(T)$ for Ce_2CuGe_3 might be caused by Schottky anomaly with spin-glass contribution.

ACKNOWLEDGMENT

This work was supported by the National Science Council of Republic of China under Contract No. NSC 88-2112-M-006-010.

[1] W. P. Beyermann, M. F. Hundley, P. C. Canfield, J. D. Thompson, M. Latroche, C. Godart, M. Selsane, Z. Fisk, and J. L. Smith, Phys. Rev. B **43**, 13 130 (1991).

[2] T. Takabatake, F. Teshima, H. Fujii, N. Nishigori, T. Suzuki, T. Fujita, Y. Yamaguchi, and Sakurai, J. Magn. Magn. Mater. **90/91**, 474 (1990).

[3] K. A. Gschneidner, Jr., J. Tang, S. K. Dhar, and A. Goldman, Physica B **163**, 507 (1990).

[4] D. Kaczorowski and H. Noël, J. Phys.: Condens. Matter **5**, 9185 (1993).

[5] Jih Shang Hwang, K. J. Lin, and Cheng Tien, Solid State Commun. **100**, 169 (1996).

[6] J. S. Hwang and C. Tien, Chin. J. Phys. (Taipei) **34**, 41 (1996).

[7] J. S. Hwang, K. J. Lin, and C. Tien, Rev. Sci. Instrum. **68**, 94 (1997).

[8] B. Chevalier, R. Pöttgen, B. Darriet, P. Gravereau, and J. Etourneau, J. Alloys Compd. **233**, 150 (1996).

[9] S. Nagata, P. H. Keesom, and H. R. Harrison, Phys. Rev. B **19**, 1633 (1979).

[10] C. A. M. Mulder, A. J. van Duyneveldt, and J. A. Mydosh, Phys. Rev. B **25**, 515 (1982).

[11] C. A. M. Mulder, Ph.D. thesis, University of Leiden, 1982.

[12] C. A. M. Mulder, A. J. van Duyneveldt, and J. A. Mydosh, Phys. Rev. B **23**, 1384 (1981).

[13] J. A. Mydosh, *Spin Glass: An Experimental Introduction* (Taylor & Francis, London, 1993).

[14] O. Sologub, K. Hiebl, P. Rogl, and O. I. Bodak, J. Alloys Compd. **227**, 37 (1995).

[15] M. B. Konyk, P. S. Salamakha, O. I. Bodak, and V. K. Pecharskii, Kristallografiya **33**, 838 (1988) [Sov. Phys. Crystallogr. **33**(4), 494 (1988)].

[16] C. Kittel, *Introduction to Solid State Physics*, 5th ed. (Wiley, New York, 1976).

[17] G. E. Brodale, R. A. Fisher, W. E. Fogle, N. E. Philips, and J. van Curen, J. Magn. Magn. Mater. **31-34**, 1331 (1983).